Supplementary Information

Unlocking Liquid Chemisorption in Solid Matrices: Immobilized Deep Eutectic Solvent–ZIF-8 Composites for Next-Generation Direct Air Capture

Yunsung Yoo[a], Xiaoliang Wang[a], Haomiao Xie[a], Geun-Ho Han[b], Ji-Yoon Song[a], Milad Ahmadi Khoshooei[a], Kent O. Kirlikovali[a], Justin M. Notestein[b], Edward H. Sargent[ae], and Omar K. Farha[abcd] *

[a]Department of Chemistry, Northwestern University, 2145 Sheridan Road, Evanston, Illinois 60208, United States;

[b]Department of Chemical and Biological Engineering, Northwestern University, 2145 Sheridan Road, Evanston, Illinois 60208, United States;

[c]International Institute of Nanotechnology, Northwestern University, 2145 Sheridan Road, Evanston, Illinois 60208, United States;

[d]Paula M. Trienens Institute for Sustainability and Energy, Northwestern University, Evanston, Illinois 60208, United States;

[e]Department of Electrical and Computer Engineering, Northwestern University, 2145 Sheridan Road, Evanston, Illinois 60208, United States.

*Corresponding author: o-farha@northwestern.edu

Section S1. Supplementary Experimental

1.1 Materials

All reagents, solvents, and gases were purchased from commercial suppliers and utilized without further modification unless otherwise specified. Alumina (Al_2O_3, particle size < 50 nm), zirconia (ZrO_2, particle size < 100 nm), and zinc nitrate hexahydrate ($Zn(NO_3)_2 \cdot 6H_2O$, ≥ 99%), were purchased from Sigma-Aldrich. Zeolite Y (SiO_2:Al_2O_3 molar ratio = 30:1), tetraethylammonium bromide (TEAB, 98%), tetraethylenepentamine (TEPA, ≥ 95%), 2-methylimidazole (99%), N,N-dimethylformamide (DMF, ≥ 99.8%) and methanol (MeOH, 99.8%) were purchased from Thermo Fisher Scientific. Ultra-high purity gases (99.999%) including N_2 and CO_2 (99.999%), used for the adsorption and desorption experiments, were provided by Airgas (Chicago, IL).

1.2 Materials Characterization

Powder X-ray diffraction (PXRD) analysis.

To investigate the crystalline structure of the solid supports and evaluate structural integrity following DES immobilization, PXRD measurements were conducted on pristine supports and the corresponding [TEAB][TEPA]$_2$@support composites. Data were collected at the Integrated Molecular Structure Education and Research Center (IMSERC) X-ray Facility at Northwestern University using a STOE-STADI-P powder diffractometer (STOE & Cie GmbH, Darmstadt, Germany) equipped with an asymmetric curved germanium monochromator and a one-dimensional silicon strip detector (MYTHEN 2 1K, DECTRIS). Cu $K\alpha_1$ radiation (λ = 1.5406 Å) was generated using a line-focused Cu X-ray source operating at 40 kV and 40 mA.

Powder samples were packed into a 3 mm metallic mask and sealed between two polyimide tape layers. Diffraction data were collected over a 2θ range of 1.5–70° with a total acquisition

time of 15 min. Prior to measurement, the instrument was calibrated using a NIST-certified silicon standard (SRM 640d).

Fourier Transform Infrared (FTIR) Spectroscopy

To confirm the successful synthesis of [TEAB][TEPA]$_2$@support composite, FTIR spectra were collected for pristine supports, pure [TEAB][TEPA]$_2$, and the resulting composites. Measurements were conducted at room temperature using a Bruker Tensor 37 FTIR spectrometer (Bruker, Billerica, MA, USA) equipped with a mid-infrared detector and a KBr beam splitter. Spectra were acquired in attenuated total reflectance (ATR) mode over the range of 4000–600 cm^{-1}, with 64 scans averaged for both sample and background. Data were acquired and processed using OPUS software, with a spectral resolution of 4 cm^{-1}.

N_2 Sorption Isotherms

Prior to N_2 sorption analysis, ZIF-8 was activated at 100 °C overnight, while Zeolite Y, alumina and zirconia were activated at 200 °C for 5 h. All [TEAB][TEPA]$_2$@support composites were pretreated at 60 °C for 10 h under dynamic vacuum before N_2 sorption measurements. Nitrogen adsorption–desorption isotherms were collected using a 3Flex surface characterization analyzer (Micromeritics, Norcross, GA, USA) at 77 K (liquid nitrogen temperature) over a relative pressure (P/P_0) range of 0.01–0.995. Pore size distributions were derived using density functional theory (DFT) assuming a cylindrical pore geometry.

CO_2 Sorption Isotherms

Prior to CO_2 sorption analysis, all materials were activated under the same conditions used for N_2 isotherm measurements. CO_2 adsorption isotherms were collected using the same 3Flex surface characterization analyzer (Micromeritics, Norcross, GA, USA) employed for N_2

measurements. Measurements were conducted at 25 °C over a pressure range of 0–1 bar, encompassing ultra-dilute (0.4 mbar) to moderate (0.15 bar) CO_2 concentrations.

CO_2 Capture–Release Cycling Stability

To evaluate the reusability of the best-performing composite, 100 consecutive CO_2 capture–release cycles were performed using a Discovery TGA5500 thermogravimetric analyzer (TA Instruments, New Castle, DE, USA). During each cycle, the sample was exposed to a gas stream containing 15% CO_2 and 85% N_2 at 30 °C for 30 minutes to facilitate CO_2 capture. Release was then carried out under 100% N_2 flow at 90 °C for 30 minutes, with a heating ramp rate of 5 °C/min. Throughout the entire process, the total gas flow rate was maintained at 25 mL/min.

The capture–release sequence was repeated for more than 100 cycles, and reusability was evaluated by tracking changes in sample mass throughout the cycling process.

X-ray Photoelectron Spectroscopy (XPS) and Depth Profiling

To investigate the surface elemental composition and chemical environments of [TEAB][TEPA]$_2$@ZIF-8 and [TEAB][TEPA]$_2$@alumina composites, XPS measurements were conducted to detect N, O, Br, and either Zn (for ZIF-8) or Al (for alumina) using a Nexsa G2 XPS system (Thermo Fisher Scientific, Waltham, MA, USA) equipped with an electron flood gun and a scanning ion gun. Measurements were carried out at room temperature at the KECK-II/NUANCE facility at Northwestern University. Samples were mounted on adhesive copper tape and analyzed using monochromated Al Kα radiation (λ = 1486.6 eV), focused to a spot size of approximately 400 μm. Spectral data was performed using Thermo Scientific Avantage software, and all binding energies were referenced to the C 1s peak at 284.8 eV.

To further examine the distribution of [TEAB][TEPA]$_2$ within the composite matrices and assess the extent of elemental diffusion into ZIF-8 and Al_2O_3 supports sputter depth profiling was performed using monoatomic Ar^+ ions at 2000 eV. Sputtering was conducted in 10 s intervals per cycle, with a total of 31 etching cycles carried out to obtain depth-resolved elemental profiles.

Scanning Electron Microscopy and Energy-Dispersive X-ray Spectroscopy (EDS)

The morphological and structural characteristics of pristine ZIF-8 and [TEAB][TEPA]$_2$@ZIF-8 composites were investigated using multiple electron microscopy techniques. Scanning electron microscopy (SEM) analysis was performed using a JSM-7900FLV field-emission SEM (JEOL Ltd., Tokyo, Japan) equipped with an energy-dispersive X-ray spectroscopy (EDS) detector at the EPIC facility (NUANCE Center, Northwestern University). Elemental mapping via EDS was performed to examine the spatial distribution of the DES phase within the composite framework. The data were acquired and processed using AZtec software (Oxford Instruments, Abingdon, UK). Samples were mounted on aluminum stubs with conductive carbon tape and coated with a 9 nm layer of OsO_4 using an OPC60A osmium coater (Filgen, Japan) to enhance surface conductivity.

Thermogravimetric analysis (TGA)

Thermogravimetric analysis was conducted to evaluate the thermal decomposition characteristics of the materials. Measurements were performed using a Discovery TGA5500 instrument (TA Instruments, New Castle, DE, USA) under a dry nitrogen atmosphere with a flow rate of 25 mL/min. Samples were heated from room temperature to 800 °C at a constant rate of 5.00 °C/min.

Inductively Coupled Plasma–Optical Emission Spectroscopy (ICP–OES)

To quantify the DES loading in the best-performing composite, zinc content was measured using inductively coupled plasma–optical emission spectroscopy (ICP–OES) with an iCAP 7600 spectrometer (Thermo Fisher Scientific, Waltham, MA, USA). Calibration standards (2.5, 5, 10, and 20 ppm) were prepared by serial dilution in Milli-Q water containing 3% nitric acid (HNO_3). Prior to analysis, the samples were digested by microwave-assisted acid digestion at 180 °C for 10 min.

Breakthrough

To evaluate the CO_2 adsorption performance of the best-performing [TEAB][TEPA]$_2$@ZIF-8 composite under dynamic capture conditions, breakthrough experiments were conducted using a BreakThrough Analyzer (Micromeritics, Norcross, GA, USA) coupled with an OmniStar® GSD 350 mass spectrometer (Pfeiffer Vacuum, Asslar, Germany). A simulated CO_2/N_2 gas mixture (15:85 v/v) was introduced at a flow rate of 5 mL/min under both dry and humid conditions, with relative humidities of 50% and 90%, respectively.

In Situ Diffuse Reflectance Infrared Fourier Transform Spectroscopy (DRIFTS)

To confirm the presence of additional CO_2 chemisorption sites introduced via immobilization of [TEAB][TEPA]$_2$ into ZIF-8, in situ DRIFTS spectra were collected using a Nicolet iS50 FTIR spectrometer (Thermo Fisher Scientific, Waltham, MA, USA) equipped with a mercury–cadmium–telluride (MCT) detector cooled by liquid nitrogen. A Harrick Scientific Praying Mantis DRIFTS accessory with a high-temperature reaction chamber was employed. Measurements were carried out under 15% CO_2 flow at 20 mL/min.

1.3 Adsorption Isotherm Modeling

Langmuir model

The Langmuir model assumes monolayer adsorption on a homogeneous surface and is expressed as:

$$q_e = \frac{q_m K_L P}{1 + K_L P} \tag{S1}$$

where q_e is the adsorbed amount (mmol/g) at pressure P (bar), q_m is the maximum monolayer adsorption capacity, and K_L is the Langmuir constant related to adsorption affinity.

For ZIF-8, the parameter q_m was constrained to ≤ 10 × $q_{m,exp}$ to avoid overfitting due to incomplete saturation.

Dual-site Langmuir model (DSL)

The dual-site Langmuir model assumes two independent adsorption sites with different affinities and capacities:

$$q_e = \frac{q_{m1} K_{L2} P}{1 + K_{L1} P} + \frac{q_{m2} K_{L2} P}{1 + K_{L2} P}$$

(S2)

where q_{m1}, q_{m2} and K_{L1}, K_{L2} are the maximum capacities and affinity constants for sites 1 and 2, respectively.

Freundlich model

This empirical model describes adsorption on heterogeneous surfaces:

$$q_e = K_F P^{1/n} \tag{S3}$$

where K_F is the Freundlich constant related to adsorption capacity, and $1/n$ is the heterogeneity index ($0 < 1/n < 1$ indicates favorable adsorption).

Sips model

The Sips model, or Langmuir–Freundlich model, accounts for surface heterogeneity and approaches saturation at high pressure:

$$q_e = \frac{q_m K_S P^n}{1 + K_S P^n} \tag{S4}$$

where q_m is the maximum capacity, K_S is the Sips affinity constant, and n is the heterogeneity parameter. When $n = 1$, the model reduces to the Langmuir equation.

Section S2. Supplementary Figures

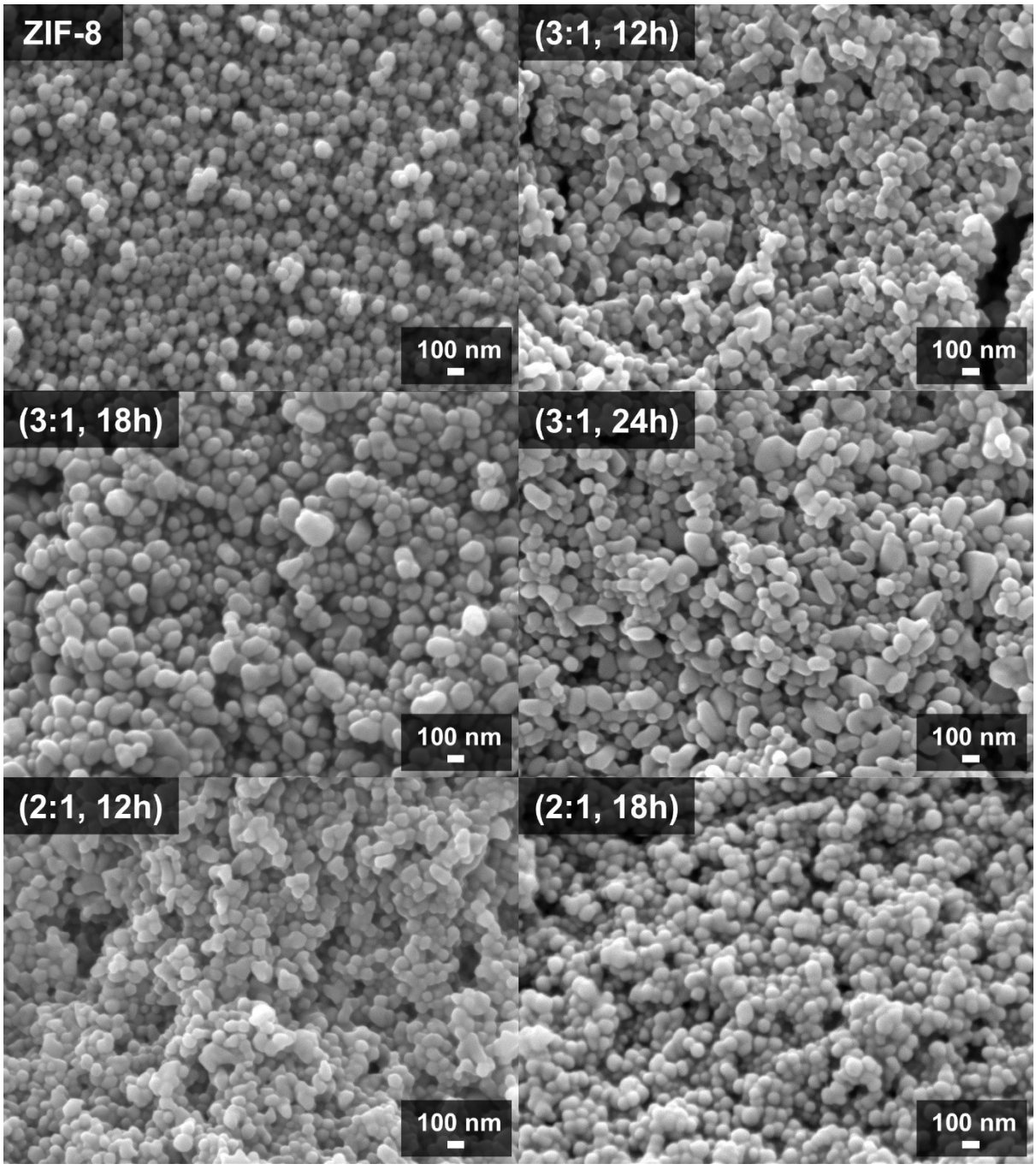

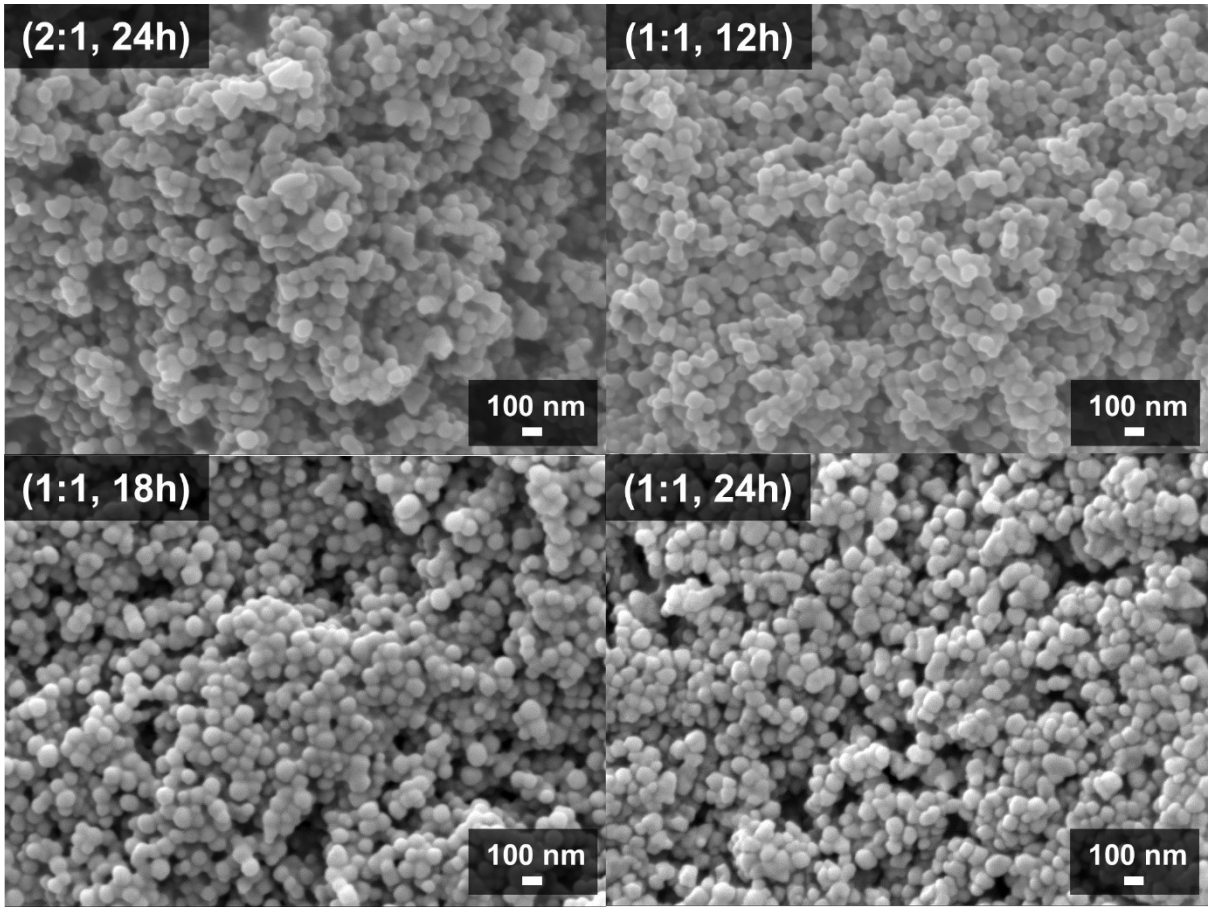

Figure S1. SEM images of pristine ZIF-8 and [TEAB][TEPA]$_2$@ZIF-8 composites prepared with varying [TEAB][TEPA]$_2$:ZIF-8 weight ratios (1:1, 2:1, and 3:1) and impregnation times (12, 18, and 24 h). All images were acquired under identical magnification; scale bar: 100 nm.

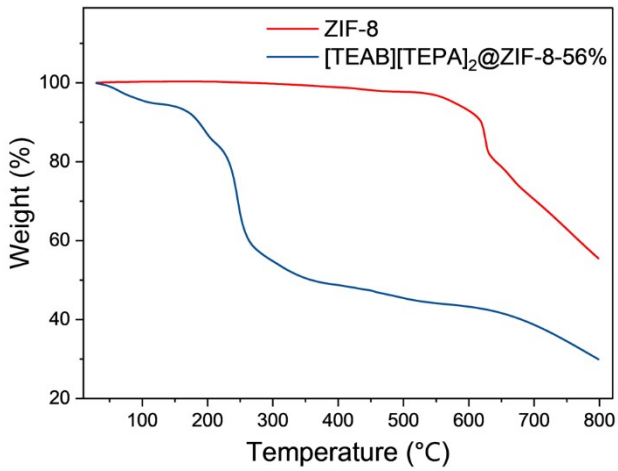

Figure S2. TGA profiles of pristine ZIF-8 and [TEAB][TEPA]$_2$@ZIF-8-56%, recorded under a dry nitrogen atmosphere with a flow rate of 25 mL/min. The samples were heated from room temperature to 800 ℃ at a constant rate of 5.00 ℃/min.

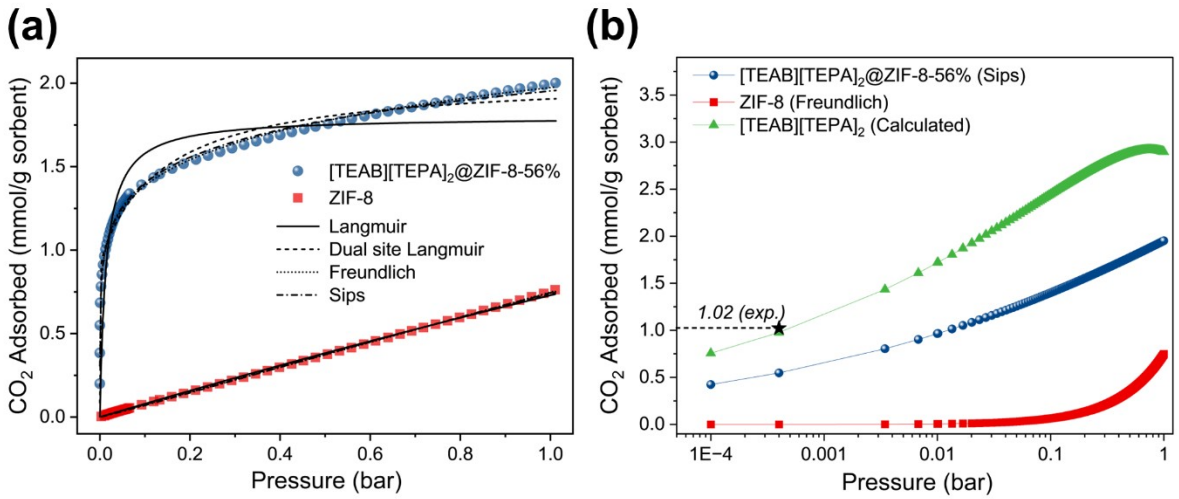

Figure S3. (a) CO_2 adsorption isotherms for pristine ZIF-8 and [TEAB][TEPA]$_2$@ZIF-8-56%, along with fitting curves based on Langmuir, dual-site Langmuir, Freundlich, and Sips models. (b) Quantitative analysis of the individual phase contributions to CO_2 uptake. Based on the known composition (56 wt% DES and 44 wt% ZIF-8), the measured uptake of the composite was normalized by the DES fraction (0.56) to estimate the specific contribution of the [TEAB][TEPA]$_2$ phase, yielding 1.02 mmol/g under the conditions tested.

For ZIF-8, the maximum adsorption capacity (q_m) in the Langmuir, DSL and Sips models was constrained to $10 \times q_{m,exp}$ (7.62 mmol/g) to prevent non-physical overestimation resulting from the lack of saturation in the experimental isotherm. This constraint is commonly applied to microporous materials exhibiting Henry-like behavior within the investigated pressure range. The isotherm of ZIF-8 displayed a nearly linear profile, and among the tested models, the Freundlich model yielded the best fit, with $1/n \approx 1$. Although this parameter lies outside the conventional "favorable" range ($0 < 1/n < 1$), it remains physically reasonable in this context, as it accurately captures the non-saturating adsorption behavior observed in ZIF-8. In contrast, the Sips model provided the best fit for the isotherm of [TEAB][TEPA]$_2$@ZIF-8–56%, indicating pressure-dependent saturation behavior on a heterogeneous adsorption surface. Although the dual-site Langmuir (DSL) model was initially expected to be suitable due to the potential presence of two distinct adsorption domains, the superior fit achieved by the Sips model suggests a more continuous distribution of adsorption site energies. In the [TEAB][TEPA]$_2$@ZIF-8–56% composite, the CO_2 uptake behavior of the immobilized DES phase was quantitatively assessed by subtracting the best-fit isotherm of pristine ZIF-8 from that of the composite. Based on this differential analysis and the known 56 wt% loading of the DES, the specific contribution of the DES phase was calculated in units of mmol/g DES. As shown in Fig. S3(b) plotted on logarithmic scales, the modeled uptake demonstrates that the immobilized DES retains substantial CO_2 adsorption capacity across a wide range of practical CO_2 partial pressures (~400 ppm to 40%). Due to the limitations of isotherm fitting at ultra-dilute concentrations, the CO_2 uptake at ~400 ppm was determined directly from experimental data, yielding 1.02 mmol/g DES.

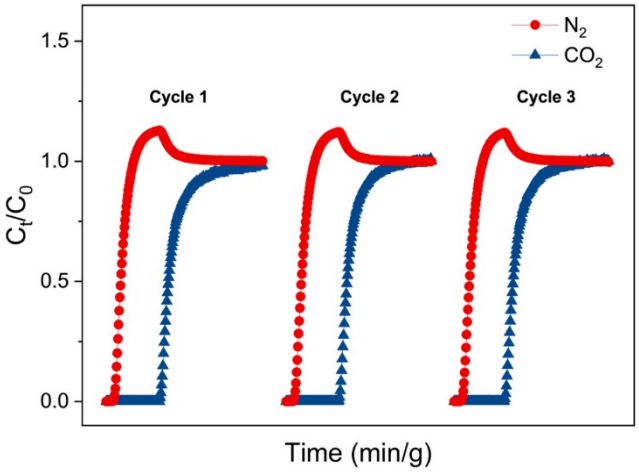

Figure S4. Breakthrough curves of [TEAB][TEPA]$_2$@ZIF-8-56% over three consecutive cycles under a binary CO_2/N_2 gas mixture (15/85, v/v) in dry conditions. The total gas flow rate was maintained at 5 mL/min, and desorption was carried out at 90 ℃.

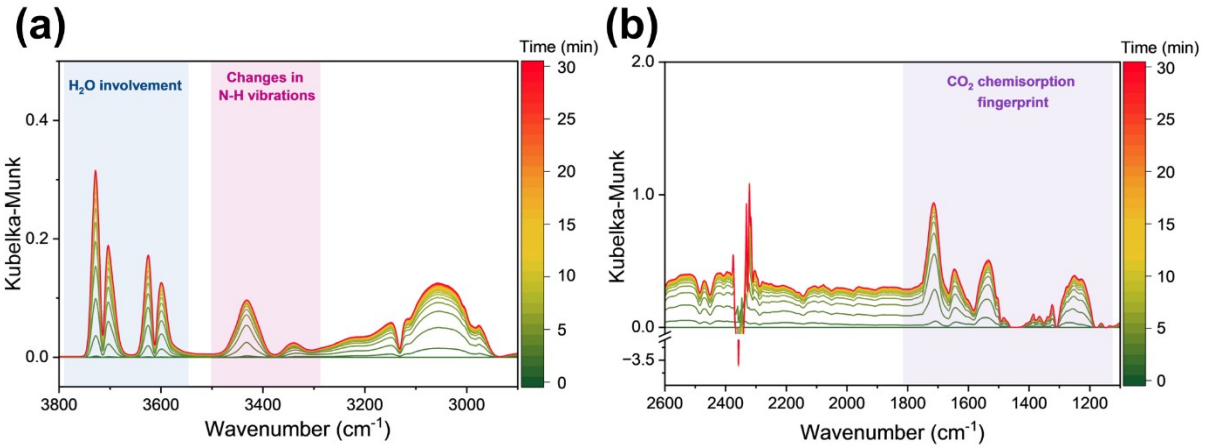

Figure S5. In situ DRIFTS analysis of [TEAB][TEPA]$_2$@ZIF-8-56% under a binary CO_2/N_2 gas mixture (15/85, v/v). (a,b) Time-resolved DRIFTS spectra collected over (a) 3800–2900 cm^{-1}, showing H_2O involvement and N–H vibrational changes, and (b) 2600–1100 cm^{-1}, highlighting CO_2 chemisorption fingerprints.

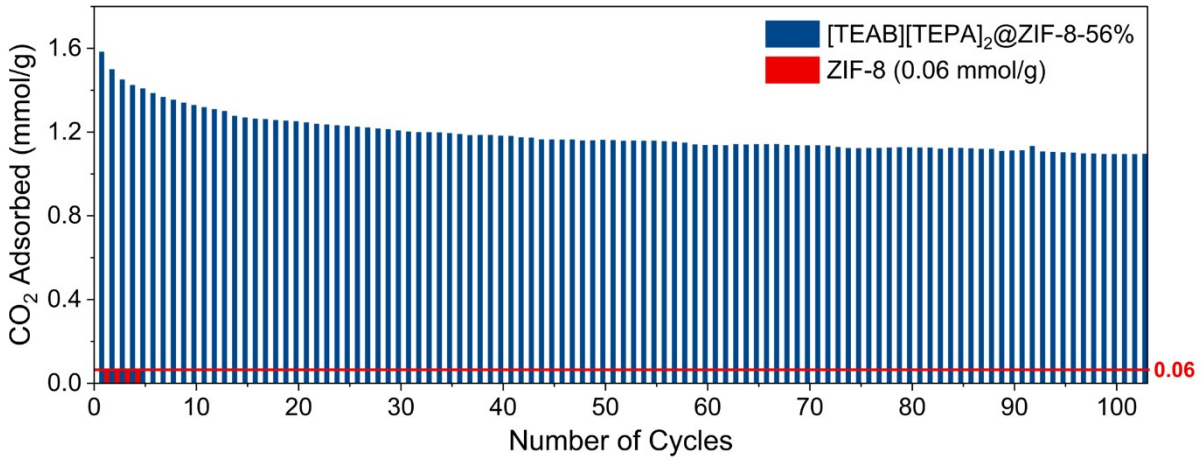

Figure S6. Cyclic CO_2 capture–release performance of [TEAB][TEPA]$_2$@ZIF-8-56% over 100 cycles and pristine ZIF-8 over 3 cycles under a binary CO_2/N_2 gas mixture (15/85, v/v). The CO_2 uptake of ZIF-8 (0.06 mmol/g) is shown as a red line. Each cycle consisted of a capture step at 30 ℃ for 30 minutes, followed by a release step under 100% N_2 at 90 ℃ for 30 minutes with a heating rate of 5 ℃/min. The total gas flow rate was maintained at 25 mL/min throughout the experiment.

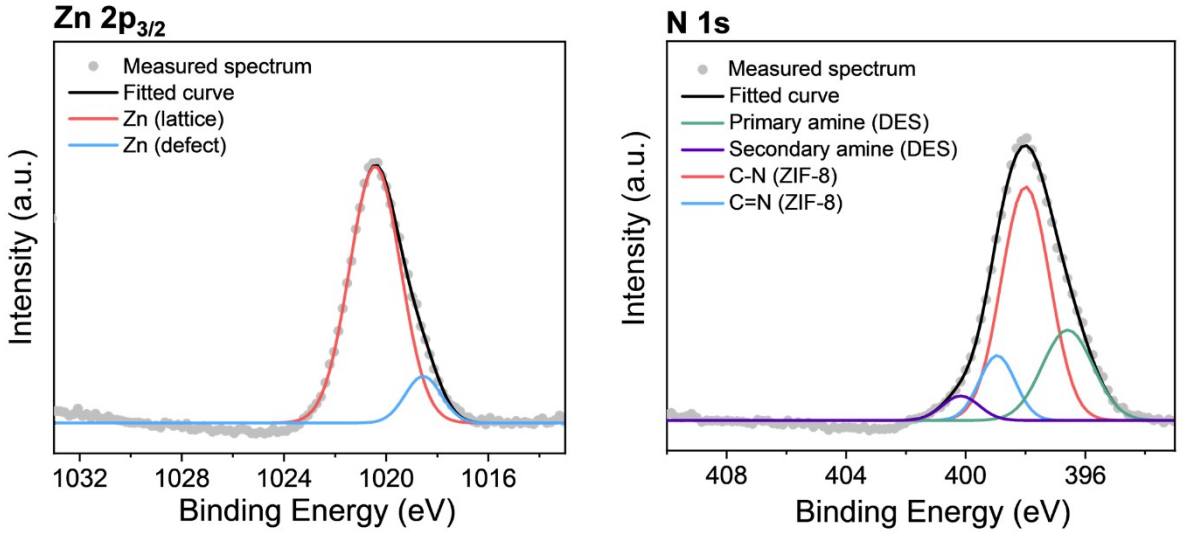

Figure S7. XPS spectra of Zn $2p_{3/2}$ and N 1s collected from the outermost surface (0 min etch) of [TEAB][TEPA]$_2$@ZIF-8-56%. All binding energies were referenced to the C 1s peak at 284.8 eV. Samples were mounted on adhesive copper tape and analyzed using monochromated Al Kα radiation (λ = 1486.6 eV) with an approximate spot size of 400 μm.

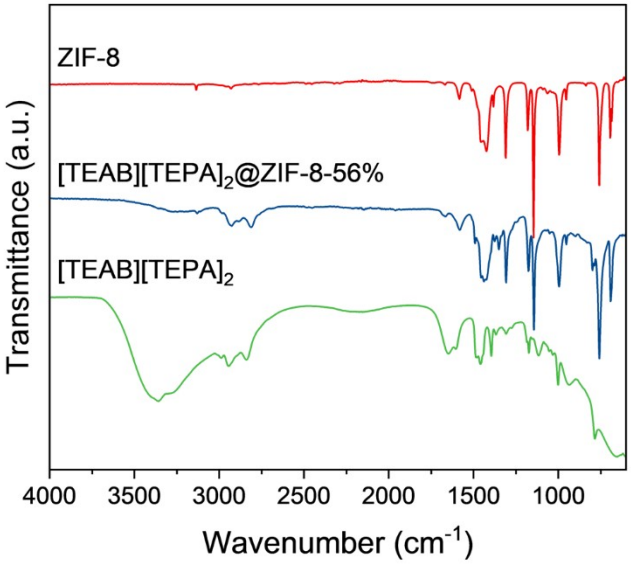

Figure S8. FTIR spectra of pristine ZIF-8, $[TEAB][TEPA]_2$, and $[TEAB][TEPA]_2$@ZIF-8-56%, collected in attenuated total reflectance (ATR) mode over the range of 4000–600 cm^{-1}. Each spectrum was acquired with 64 scans averaged for both sample and background at a resolution of 4 cm^{-1}.

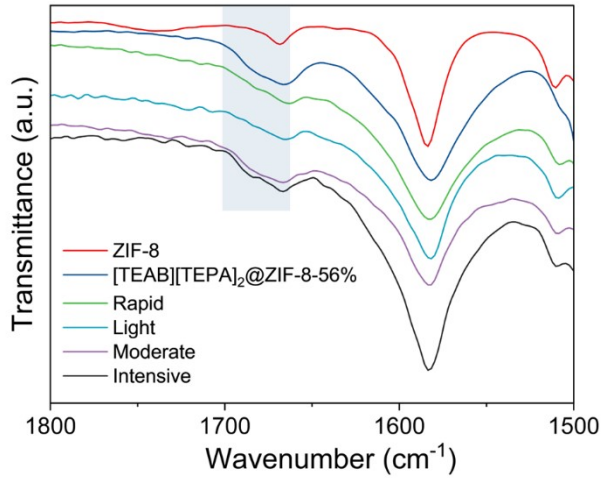

Figure S9. FTIR spectra of washed [TEAB][TEPA]$_2$@ZIF-8-56% in four distinct washing protocols: : (1) rapid, involving immediate rinsing with 50 °C DMF; (2) light, consisting of three 10-minute soakings; (3) moderate, consisting of three 1-hour soakings; and (4) intensive, involving three soakings carried out over the course of a full day—all performed at 50 °C over the range of 4000–600 cm^{-1}. Each spectrum was acquired with 64 scans averaged for both sample and background at a resolution of 4 cm^{-1}.

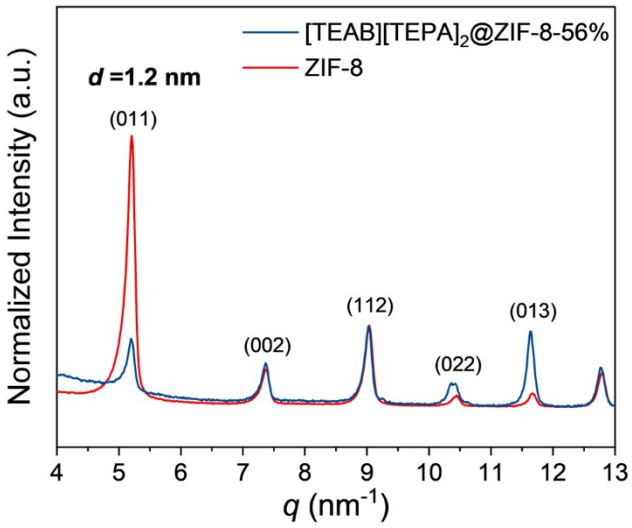

Figure S10. PXRD patterns of pristine ZIF-8 (red) and [TEAB][TEPA]$_2$@ZIF-8-56% composite (blue), plotted as scattering vector (q, nm^{-1}) versus normalized intensity. All patterns were normalized to the intensity at q = 9 nm^{-1} to enable consistent comparison.

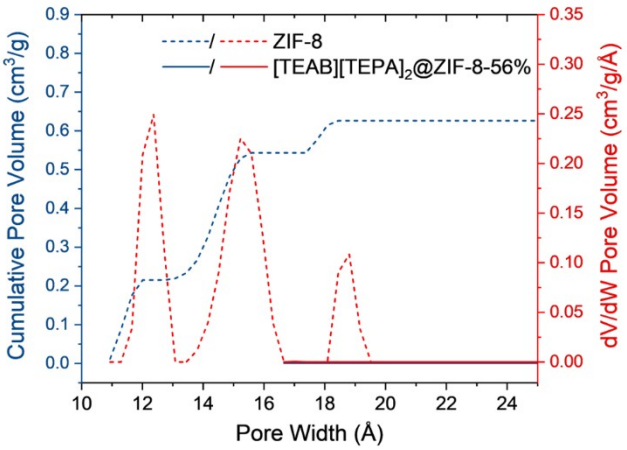

Figure S11. Pore size distribution curves of pristine ZIF-8 (dashed line) and [TEAB][TEPA]$_2$@ZIF-8-56% composite (solid line). The distributions were calculated using density functional theory (DFT) assuming a cylindrical pore geometry. Cumulative pore volume (blue) is plotted on the left y-axis, while differential pore volume (dV/dW, red) is shown on the right y-axis.

S3. Supplementary Tables

Table S1. Fitted parameters of adsorption isotherm models (Langmuir, dual-site Langmuir, Freundlich, and Sips) for CO_2 adsorption on ZIF-8 and $[TEAB][TEPA]_2$@ZIF-8-56% at 25 °C over a pressure range of 0–1 bar.

Models	**Parameters**	**Materials**	
		ZIF-8[a]	**$[TEAB][TEPA]_2$@ ZIF-8-56%**
Langmuir	q_m (mmol/g)	7.617	1.799
	K_L (1/bar)	0.106	71.728
	R^2	0.9981	0.8125
	%AAD	3.88	14.37
Dual site Langmuir	q_{m1} (mmol/g)	7.603	0.941
	K_{L1} (1/bar)	0.0511	5827.156
	q_{m2} (mmol/g)	7.602	1.101
	K_{L2} (1/bar)	0.0510	7.093
	R^2	0.9994	0.9810
	%AAD	2.68	4.85
Freundlich	K_F	0.749	1.97421
	1/n	1.006	0.154
	R^2	0.9999	0.9948
	%AAD	2.09	2.81
Sips	q_m (mmol/g)	7.617	5.939
	K_S (1/bar)	0.124	0.0286
	n	1.065	0.201
	R_2	0.9997	0.9964
	%AAD	2.81	2.13

a) For completeness, Langmuir, Sips, and DSL models were fitted using bounded optimization with $q_m \leq 10 \times q_{m,\,exp.}$

Table S2. Comparison of FTIR peak positions for [TEAB][TEPA]$_2$, pristine ZIF-8, and [TEAB][TEPA]$_2$@ZIF-8-56%. All values are in cm^{-1}. Values in parentheses indicate the wavenumber shift relative to the corresponding pristine component.

[TEAB][TEPA]$_2$	**[TEAB][TEPA]$_2$@ ZIF-8-56%**	**ZIF-8**	**[TEAB][TEPA]$_2$@ ZIF-8-56%**
3355	3354 (-1)	3136	3129 (-7)
3276	3272 (-4)	2930	2923 (-7)
2990	2982 (-8)	2767	2761 (-6)
2944	2939 (-5)	2695	2684 (-11)
2890	2879 (-11)	2488	2480 (-8)
2839	2810 (-29)	2454	2450 (-4)
1647	1665 (+18)	1739	1739
1602	1605 (+3)	1668	1668
1486	1492 (+6)	1583	1580 (-3)
1478	1478	1509	1504 (-5)
1459	1454 (-5)	1457	1455 (-2)
1442	1440 (-2)	1424	1424
1395	1396 (+1)	1382	1376 (-7)
1367	1374 (+7)	1310	1308 (-2)
1308	1308	1179	1176 (-3)
1274	1272 (-2)	1146	1144 (-2)
1185	1188 (+3)	1090	1082 (-8)
1174	1172 (-2)	1065	1069 (+4)
1002	1008 (+6)	994	993 (-1)
936	938 (+2)	954	954
797	797	839	837 (-2)
783	788 (+5)	759	760 (+1)